medRxiv preprint doi: https://doi.org/10.1101/2023.12.30.23300671; this version posted December 31, 2023. The copyright holder for this preprint **(which was not certified by peer review)** is the author/funder, who has granted medRxiv a license to display the preprint in perpetuity.
It is made available under a CC-BY-ND 4.0 International license .

Molecular insights of β-lactams resistance in *Klebsiella pneumoniae* isolates with focus on multidrug resistance and virulence from colonization samples

Lavouisier F.B. Nogueira [1, 2 #], Marco A.F Clementino [1, 2 #], Marília S. Maia [1, 2#], Ila F.N. Lima [3], Jorge L.N. Rodrigues [3], Luciana V.C. Fragoso [3], Glairta S. Costa [3], Jose Q.S. Filho [1], Alexandre Havt [1, 2], Deiziane V.S. Costa [4], José K. Sousa [1], Lyvia M.V.C. Magalhães [1], Dilza Silva [5], Nicholas E. Sherman [5] and Aldo A.M. Lima [1, 2 *]

[1] Institute of Biomedicine, Faculty of Medicine, Federal University of Ceara, Fortaleza-Ceara 60430-270, Brazil.
[2] Postgraduate Medical Microbiology Program, Department of Medicine, Federal University of Ceara, Fortaleza-Ceara 60430-270, Brazil.
[3] Hospital Universitário Walter Cantídio, Federal University of Ceara, Fortaleza-Ceara 60430-270, Brazil.
[4] Infectious Diseases and International Health, University of Virginia, Charlottesvillle, VA 22908.
[5] Biomolecular Analysis Facility, School of Medicine, University of Virginia, Charlottesvillle, VA 22908.
***** Correspondence: alima@ufc.br
[#] These authors contributed equally to this work.

e-Mails: lavouisier@gmail.com, mclementino@ufc.br, mmaia800@gmail.com, ila.lima@ebserh.gov.br, jorge1207@gmail.com, luciana.vladia@gmail.com, glairta14@gmail.com, jquirinof@gmail.com, ahavt@ufc.br, deiziane2009@gmail.com, kleybson.jks@alu.ufc.br, lyviacarneiro@ufc.br, xjb8bf@virginia.edu, nes3f@virginia.edu, alima@ufc.br.

Abstract: *Klebsiella pneumoniae* is associated with high resistance to antimicrobials and is common in isolates from colonization and nosocomial infections. The study aims to detect resistance genes belonging to the *bla* family and investigate metabolic pathways in *K. pneumoniae* isolates. Genes from the subfamilies included: *blaSHV, blaTEM, blaNDM, blaKPC, blaGES, blaCTX-M* and relevant variants of the *blaOXA* subfamily. Mass spectrometry data were acquired on the Orbitrap IDX spectrometer (Thermo) connected to the Vanquish UPLC system. Isolates from 122 *K. pneumoniae* samples were collected from 04/23/2019 to 05/29/2021. A high prevalence of resistance to penicillins, cephalosporins and carbapenems was found among the isolates. The identified genotypic profile showed a high prevalence of genes belonging to Ambler's classes of beta-lactamases A, B and D. In the metabolomic study, the N-fructosyl isoleucine metabolite was identified increased in multidrug-resistant (MDR) strains of *K pneumoniae* compared to strains susceptible to antimicrobials. In conclusion, the assays developed were efficient in detecting the main genes of the *bla* family of resistance in *K. pneumoniae*. The use of the pentose phosphate metabolic pathway suggests the regulation of bacterial growth, virulence, and colonization in MDR *K. pneumoniae* strains.

Keywords: Antimicrobial resistance; multidrug-resistant; β-lactamases; qPCR; molecular diagnosis; virulence; *Klebsiella pneumoniae*.

---

1. Introduction

Bacterial resistance to antimicrobial agents is a global public health problem that leads to an increase in the cost of treatment, length of stay and morbidity and mortality of hospitalized patients, especially in intensive care units (ICU) [1, 2]. In this sense, understanding the emergency mechanisms of regulation and dissemination of resistance to antimicrobial agents in the pathogenesis of bacterial colonization and/or infection can be of critical importance in preventing and controlling this dissemination.

NOTE: This preprint reports new research that has not been certified by peer review and should not be used to guide clinical practice.

Klebsiella pneumoniae is a gram-negative γ-proteobacteria microorganism belonging to the *Enterobacteriales* family, and is known to be opportunistic, carrying several virulence factors and capable of

medRxiv preprint doi: https://doi.org/10.1101/2023.12.30.23300671; this version posted December 31, 2023. The copyright holder for this preprint (which was not certified by peer review) is the author/funder, who has granted medRxiv a license to display the preprint in perpetuity.
It is made available under a CC-BY-ND 4.0 International license .

accumulating resistance genes to various classes of antimicrobials. It is commonly related to cases of colonization and/or healthcare-associated infections (HAIs) and has been identified as an etiological agent in pneumonia, urinary tract infections (UTI), soft tissue and surgical wound infections, bacteremia, and sepsis [3]. It is estimated that *K. pneumoniae* is responsible for approximately 10% of all cases of nosocomial infections, and of these, 32.8% are caused by strains resistant to multiple antimicrobial drugs. However, studies indicate that the rate of isolated strains presenting resistance to antimicrobials has increased over the years [4, 5]. *K. pneumoniae* has been associated with the ability to overcome colonization resistance imposed by the gastrointestinal microbiota [6] and has been reported as an emerging multidrug-resistant strain and of emergency priority by the World Health Organization (WHO) for the development of new therapies [7]. Epidemiological data have demonstrated that *K. pneumoniae* can translocate from the gastrointestinal tract to other sterile sites of the same host or other patients through the fecal-oral route. Despite the well-established clinical relevance, little is known about the mechanisms behind the emergence and dissemination of multidrug-resistant (MDR) *K. pneumoniae* strains [8].

One of the most likely causes of the increasingly frequent appearance of bacterial strains resistant to one or more antibiotics is the excessive and sometimes incorrect use of antimicrobials. The relatively long time required to identify the pathogen by traditional methods, as well as for the results of the antimicrobial susceptibility test (AST), forces the clinician to use broad-spectrum drugs empirically, increasing selective pressure, the which ends up benefiting pathogens genetically capable of adapting to the adverse environment [1, 9]. A possible answer to reduce the time needed to obtain a resistance profile is the development of molecular methodologies, which aim to identify the genetic profile of resistance of the agent causing the infection. Molecular laboratory tests could not only make the identification of resistance faster, but they could also be more susceptible and useful in the case of colonization and/or infections caused by fastidious microorganisms, giving the clinician a timely response to reduce the empirical use of antimicrobial drugs [10]. Beta-lactams are the class of antimicrobials most affected by resistance in general, which is conferred in gram-negatives, mainly by the *bla* gene family [11, 12, 13]. Therefore, we seek to develop a molecular assay, capable of identifying all variants of the most relevant genes of the bla family, these being: *blaSHV, blaTEM, blaNDM, blaKPC, blaGES, blaCTX-M*. In addition to variants with epidemiology most relevant components of the *bla-OXA* gene. Thus, creating a set of primers capable of detecting the presence of hundreds of resistance genes with a reduced number of reactions.

In this study, we identified the phenotypic and genotype profile of genes from the *bla* family of β-lactamases in MDR *K. pneumoniae* strains isolated from patients admitted to the ICU in Fortaleza-CE, Brazil. Furthermore, we investigated the metabolomic modulation associated with virulence in MDR strains of *K. pneumoniae* compared with strains susceptible to antimicrobial agents of *K. pneumoniae*, both isolated from colonization sites.

2. Materials and Methods

2.1 Obtaining bacterial isolates and identification.

This study was a cohort prospective design. It was approved by the Brazilian National Research Ethics Commission (no. 03300218.2.0000.5054), and carried out in the University Hospital, Federal University of Ceará, Fortaleza, Northeastern Brazil. For the following study, samples were collected to investigate colonization sites, as part of the clinical investigation of patients admitted to the ICU of a tertiary care health unit in the city of Fortaleza-CE. We included those microorganisms that were identified as gram-negative bacteria, resistant to two or more groups of antimicrobial agents, including subclasses of β-lactams, fluoroquinolones,

medRxiv preprint doi: https://doi.org/10.1101/2023.12.30.23300671; this version posted December 31, 2023. The copyright holder for this preprint (which was not certified by peer review) is the author/funder, who has granted medRxiv a license to display the preprint in perpetuity.
It is made available under a CC-BY-ND 4.0 International license .

aminoglycosides, macrolides, and glycopeptides. Bacterial isolates were selected from bloodstream, as well as other sites considered noble, such as cerebrospinal fluid (CSF), pleural, peritoneal, pericardial, synovial, among others. Bacterial isolates from urinary tract, bronchoalveolar lavage, tracheal aspirate, sputum, abscess drainage, surgical wounds, among others, were also selected. Culture of fragments, such as skin, organs, and bones as well as rectal swab culture for surveillance, without apparent infection also had their bacterial isolates selected. With the aim of diagnosing potential etiological agents, blood culture samples and other noble liquids were inoculated in specific bottles and incubated in the BacT/Alert® 3D equipment (BioMérieux, Marcy l'Etoile, France). The other biological materials were culture using a qualitative or quantitative sowing technique, to obtain isolated colonies. The plates were incubated at 37 ± 2°C for 18-24 hours [14].

The bacterial isolates were identified and tested for their susceptibility to antimicrobials using the automated VITEK® 2 Compact method (BioMérieux, Marcy l'Etoile, France), according to the manufacturer's recommendations. Minimum inhibitory concentrations were interpreted according to the Clinical and Laboratory Standards Institute (CLSI). For quality control of sensitivity tests, strains from the American Type Culture Collection (ATCC) were used. Specimens that had a resistance profile that fit the research objectives were included in the study.

2.2 Extraction of bacterial DNA.

To extract the genetic material, the Wizard Genomic DNA Purification extraction and purification kit (Promega, Madison, USA) was used, according to the manufacturer's recommendations.

After extraction, all samples were then quantified by spectrophotometry using the NanoDropTM 2000 (Thermo Fisher Scientific, Waltham, Massachusetts, USA) and stored in a -80°C freezer until used in the experiments.

2.3 Selection of genes used in the study and obtaining FASTA sequences.

For greater coverage of the genetic profile of resistance to β-lactams in gram negatives, genes with relevant prevalence epidemiology, belonging to the *bla* gene family, were part of the study, and these included the genes*: blaSHV, blaTEM, blaNDM, blaKPC , blaGES, blaCTX-M and blaOXA*. The sequences used were obtained through the Comprehensive Antibiotic Resistance Database (CARD) platform, which compiles and organizes the resistance gene sequences available in GenBanck, and the list of identifiable sequences is available in the supplementary material Text S1.

2.4 Primer design

To design the primers, all variant sequences of each gene included in the study available on the CARD platform were gathered, the sequences were aligned using the Clustal Omega software, and the alignments were analyzed using the SnapGene software.

Consensus regions with homology ⩾95% were selected and these were used to design the primers using the Primer Blast platform from the National Center for Biotechnology and Information (NCBI, USA). The consensus sequences obtained are available in the supplementary material Text S2.

Genes with few conserved regions, for which it was not possible to obtain consensus sequences with homology ⩾95%, were separated into clades, and primers were then designed for the sequences by phylogenetic grouping, complying with a minimum of 95% similarity.

medRxiv preprint doi: https://doi.org/10.1101/2023.12.30.23300671; this version posted December 31, 2023. The copyright holder for this preprint (which was not certified by peer review) is the author/funder, who has granted medRxiv a license to display the preprint in perpetuity.
It is made available under a CC-BY-ND 4.0 International license .

2.5 *In silico* validation of the developed primers

All primers developed were validated *in silico* regarding their specificity, structure, formation of primer-dimers and hairpins using the Primer-BLAST® (NCBI, USA) and Sequence Manipulation Suite (SMS): PCR Primer Stats platforms.

2.6 Testing, optimization, and standardization of primers

The reactions were standardized with the use of positive controls developed in-house, through amplification of genetic material, isolation, and purification of amplicons, originating from isolates phenotypically resistant to beta-lactams, and negative control (water DNase/RNase free). They were carried out using a CYBR Green master mix (Promega, Madison, USA), the initial results were evaluated regarding the melting temperature (Tm), to confirm the specificity of the amplicons.

To determine the most efficient qPCR conditions, to reduce the existence of non-specificity and facilitate the interpretation of the results, the concentration gradient and annealing temperature (Ta) of the primers were performed. The qPCR reaction conditions included a hot start step at 95°C for 2 minutes, followed by 35 cycles consisting of a denaturation step for 15 seconds at 95°C, and an annealing/extension step for 1 minute at RT. specific to each primer, all reactions went through a final melting curve step, with a temperature variation of 60 to 95°C with an increase of 0.05°C/sec.

A 9-point efficiency curve was performed with a dilution factor of 1:8, for each primer developed, with concentrations ranging from ≈27,438,596 to ≈2 (copies/µL), through this procedure it was possible to determine the values of threshold, evaluate the efficiency (%), the correlation coefficient (R^2) and the limit of detection of each primer.

2.7 Detection of resistance-related genes by molecular biology

The *K. pneumoniae* isolates obtained in the study were tested against the developed primers. Melting curve analysis of all reactions was used to evaluate the specificity of the results of the isolates in comparison to the specific melting temperature (Tm) of the positive control.

2.8 Methodology for collecting susceptible and resistant *Klebsiella pneumoniae* samples.

Samples of *K. pneumoniae* susceptible and multidrug resistant to antimicrobial agents were collected from patients hospitalized between April 23, 2019, and May 29, 2021, in the Intensive Care Unit of the University Hospital, Faculty of Medicine, UFC, and they were submitted for metabolomic analysis. For this experiment, seven samples of the culture supernatant were designed: one sample of the culture medium, two samples of the culture supernatant of susceptible *K. pneumoniae* (biological replicates), four samples of the culture supernatant of multidrug-resistant *K. pneumoniae* (MDR) for untargeted metabolomics determination and analysis. Samples of the intracellular medium of the *K. pneumoniae* culture, two samples of susceptible *K. pneumoniae* (biological replicates) and four samples of MDR *K. pneumoniae* were also used for untargeted metabolomic analysis. Technical replicates were performed for susceptible media and samples to allow for a pilot statistical comparison.

2.9 Methodology for extracting *K. pneumoniae* culture supernatant.

To 200 µL of *K. pneumoniae* culture medium or control medium, 800 µL of 80% methanol was added at -20 ºC. The samples were vortexed and incubated at -20°C for 2 hours for protein precipitation. The samples were centrifuged for 10 min at 4°C at 10,000 g (Benchtop refrigerated centrifuge 10k RPM Eppendorf) and the supernatants were transferred to new tubes. The samples were dried under vacuum (Speed Vac

medRxiv preprint doi: https://doi.org/10.1101/2023.12.30.23300671; this version posted December 31, 2023. The copyright holder for this preprint (which was not certified by peer review) is the author/funder, who has granted medRxiv a license to display the preprint in perpetuity.
It is made available under a CC-BY-ND 4.0 International license .

Thermo fisher) for approximately 4-5 hours. Dried samples were redissolved in 100 µL of 0.1% formic acid in water containing Metabolomics QReSS labeled heavy standards diluted 100X. (https://www.isotope.com/userfiles/files/assetLibrary/MET_RSCH_QReSS.pdf). A quality control (QC) was done, combining 10 µL of each sample. After the QC test in the mass spectrometer, the samples were diluted 10x to be analyzed. The injection volume of each sample was 10 µL per ionization mode.

2.10 Methodology for extractions from the intracellular medium of *K. pneumoniae* culture

To each tube, 750 µL of cold chloroform:methanol (2:1) mixture at -20 ºC was added, vortexed and transferred to tubes reinforced with a ball beater. Cells were disrupted in a bead beater with steel balls for 3 min at an intensity of 5 (Bead Ruptor Elite Omni International Material). The tubes were shaken vigorously for 30 min at 4°C in a temperature-controlled thermal shaker (Thermomixer Eppendorf). 400 µL of water was added, shaken vigorously, and centrifuged for 10 min at 10,000 rpm (Benchtop refrigerated centrifuge 10k RPM Eppendorf) for phase separation. The upper aqueous/methanolic phase was saved as a mixture of soluble metabolites and transferred to Eppendorf tubes. Soluble metabolites were dried under vacuum for 3-4 h (Speed Vac Thermo Fisher). Before running, samples were reconstituted in 100 µL of 0.1% formic acid in water containing 100X diluted Metabolomics QReSS labeled heavy standards (https://www.isotope.com/userfiles/files/assetLibrary/MET_RSCH_QReSS.pdf). The QC sample was prepared with 10 µL of each sample. The injection volume of each sample was 10 µL.

2.11 Analysis by Ultra Performance Liquid Chromatography Coupled to Tandem Mass Spectrometry (UPLC-MS/MS) of metabolites.

MS data were acquired on the Orbitrap IDX spectrometer (Thermo) connected to the Vanquish UPLC system. Soluble metabolites were separated using a Waters BEH C18 column (100 x 2.1 mm, 1.9 µm) operated at 30 °C and a flow rate of 250 µL/min. Mobile phase A was 0.1% formic acid in water and mobile phase B was 0.1% formic acid in 90% methanol. Bulk scan range: 67-1000 at 120,000 resolutions with 0.6 sec scan range. The 10 most intense ions in each full scan were selected for fragmentation and MS2 spectra were acquired at a resolution of 30,000 and scaled collision dissociation fragmentation energy of 25, 30, 35 was used.

2.12 UPLC gradient

The total time used in the UPLC gradient runs was 15 minutes. The flow used was 0.250 mL/min and the following gradient in the percentage of mobile phase B was 50% at 8 min, 98% at 9 min. maintaining until a time of 13 min., ending with 0% between a time of 13.1 – 15 min.

2.13 Verification settings in the mass spectrum

The configurations used in the verification through the mass spectrum were orbit trap of the mass spectrum in the master scan, with an orbitrap detector with a resolution of 120,000. We used quadrupole isolation with a scanning range between 67-1000 m/z, using the frequency lens at 60%. The automatic gain control target was customized and normalized to 25%. The maximum injection time mode has been customized with a maximum injection time of 50 ms. MIcroscans of 1 and profile with positive polarity. Font fragmentation has been disabled.

medRxiv preprint doi: https://doi.org/10.1101/2023.12.30.23300671; this version posted December 31, 2023. The copyright holder for this preprint **(which was not certified by peer review)** is the author/funder, who has granted medRxiv a license to display the preprint in perpetuity.
It is made available under a CC-BY-ND 4.0 International license .

2.14 Data acquisition, metabolic identification, and data analysis.

Once the data was acquired, the samples were analyzed using the open-source software MS-DIAL. More details about the software can be obtained here: http://prime.psc.riken.jp/compms/msdial/main.html [15,16]. Three blank samples were included in the analysis to identify background ions and remove them later. Samples acquired using MS1 full scan used for quantification and data-dependent acquisition (DDA) mode were used for spectral identification of metabolites. Tolerance MS1 was set to 0.01 Da and MS2 set to 0.025 Da. For peak harvesting, the mass slice width was set to 0.1. For peak alignment, the maximum retention time tolerance was set at 0.5 min, the MS1 tolerance was set at 0.01. Peaks were identified by searching MS2 spectra in the public MS-DIAL database downloaded in January 2023 (324,191 records for positive mode and 64,669 entries for negative mode) using a mass tolerance of 0.01 Da for MS1 and 0.05 Gives to MSMS with an identification cutoff point of 80% http://prime.psc.riken.jp/compms/msdial/main.html#MSP. Additionally, peaks were also searched against the core Biomolecular Analysis Facility's internal IROA library (both positive and negative mode) with a mass tolerance of 0.02 and identification cutoff of 85%. The data was manually inspected and identifications without MS2 were filtered, except for identifications of the IROA molecule.

3. Results

3.1. Selection of bacterial samples

A total of 249 samples of gram-negative bacteria resistant to beta-lactam antimicrobials, fluoroquinolones, aminoglycosides, macrolides and glycopeptides were identified, among which the most prevalent microorganism was *Klebsiella pneumoniae* 48.99% (122/249).

3.2. Identification of the phenotypic profile of beta-lactams resistance of *K. pneumoniae* strains

The bacteria isolates included in the study were tested against a wide range of beta-lactams drugs, and the presence of a high percentage of isolates resistant to these drugs was verified, which included penicillins: ampicillin (100.00%), ampicillin/sulbactam (92.00%) and piperacillin/tazobactam (88.46%), cephalosporins: cefepime (83.02%), cefoxitin (73.68%), ceftazidime (86.54%), ceftazidime/avibactam (11 .76%), ceftriaxone (83.02%), cefuroxime (90.38%) and cefuroxime axetil (81.82%) and carbapenems: ertapenem (44.00%), imipenem (71.70%) and meropenem (69.81%), as shown in **Figure 1**.

medRxiv preprint doi: https://doi.org/10.1101/2023.12.30.23300671; this version posted December 31, 2023. The copyright holder for this preprint **(which was not certified by peer review)** is the author/funder, who has granted medRxiv a license to display the preprint in perpetuity.
It is made available under a CC-BY-ND 4.0 International license .

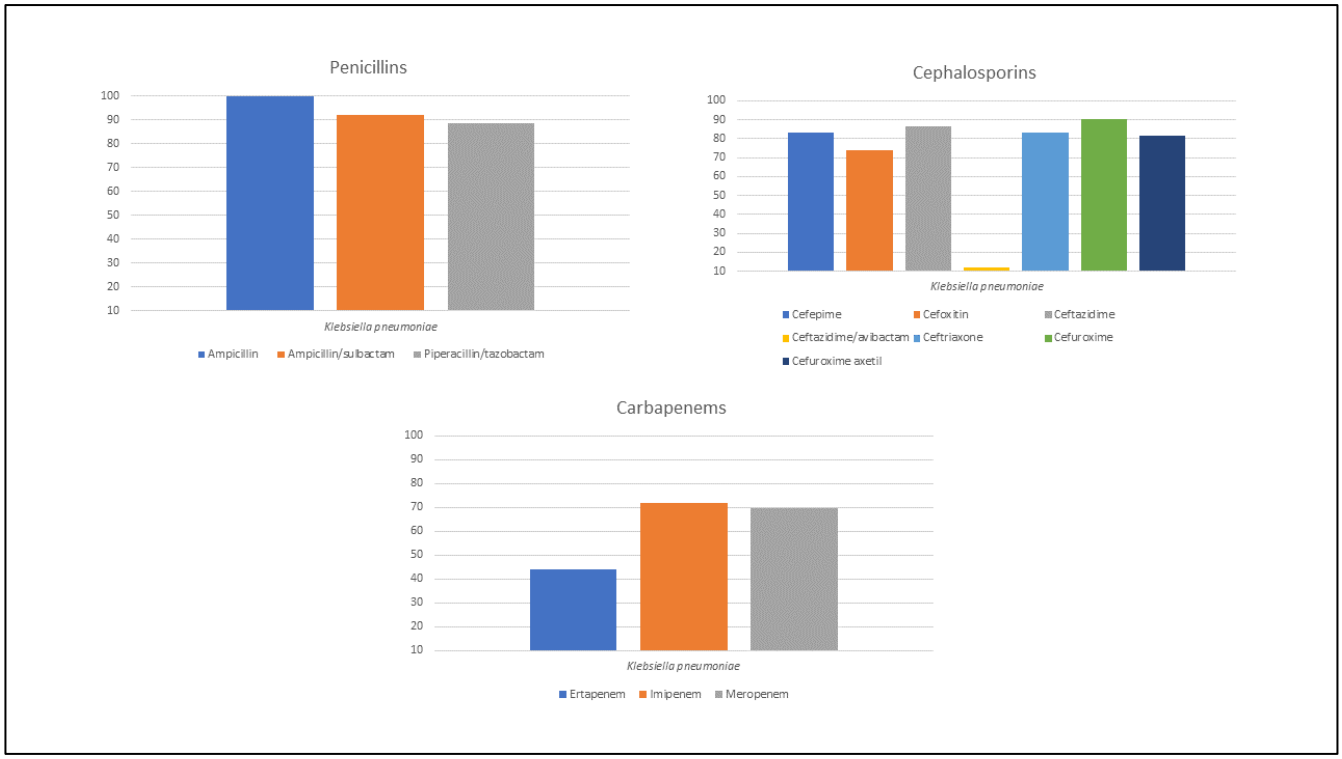

Figure 1. Prevalence of *K. pneumoniae* isolates resistant to the beta-lactams evaluated (Penicillins, Cephalosporins and Carbapenems), demonstrating a phenotypic profile of resistance to multiple beta-lactams drugs, in more than 70% of the isolates, with the exception of ceftazidime/avibactam and ertapenem.

3.3. Primers design

After selection on the Comprehensive Antibiotic Resistance Data-base (CARD) platform and subsequent compilation and analysis of FASTA sequences, it was possible to identify consensus sequences common to all sequences available in the database (CARD) for each of the genes included in the study: *blaSHV* (N = 156), *blaTEM* (N = 167), *blaNDM* (N = 27), *blaKPC* (N = 19), *blaGES* (N = 25), and *blaCTX-M* (N = 144). Except for the *blaOXA* gene, for which the most clinically relevant sequences were used (N = 203).

The *blaCTX-M* and *blaOXA* genes, due to their diversity and high degree of genetic variation between homologous sequences, were grouped into clades, and divided into *CTX-M* 1 (N = 42), *CTX-M* 2 (N = 16), *CTX-M* 3 (N = 49), *CTX-M* 4 (N = 14) and *CTX-M* 5 (N = 23), while the *blaOXA* gene was divided into the *OXA-23* like groups (N = 25), *OXA-24/40 like* (N = 8), *OXA-48 like* (N = 17) and *OXA-51 like* (N = 153), as can be seen in **Figures 2** and **3**.

medRxiv preprint doi: https://doi.org/10.1101/2023.12.30.23300671; this version posted December 31, 2023. The copyright holder for this preprint **(which was not certified by peer review)** is the author/funder, who has granted medRxiv a license to display the preprint in perpetuity.
It is made available under a CC-BY-ND 4.0 International license .

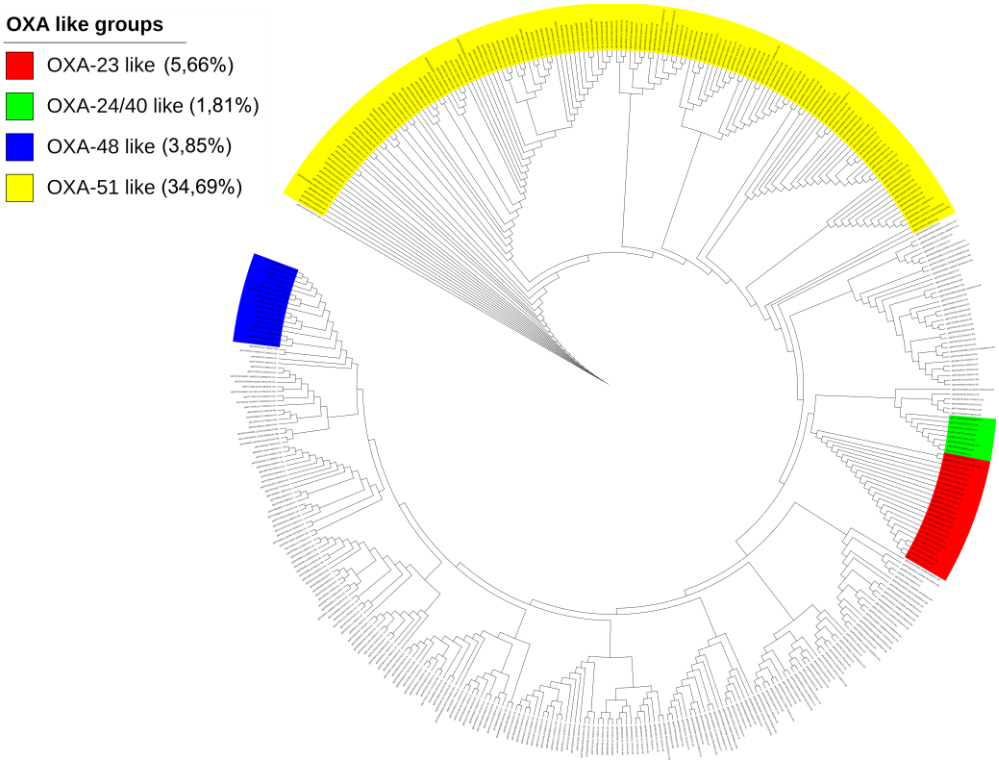

Figure 2. Cladogram of the *blaOXA* subfamily showing the most epidemiologically relevant groups, covered by the primers developed, and the percentage of sequences identifiable by each primer in comparison with the total number of the *blaOXA* family (N = 441) at the time of publication of this work.

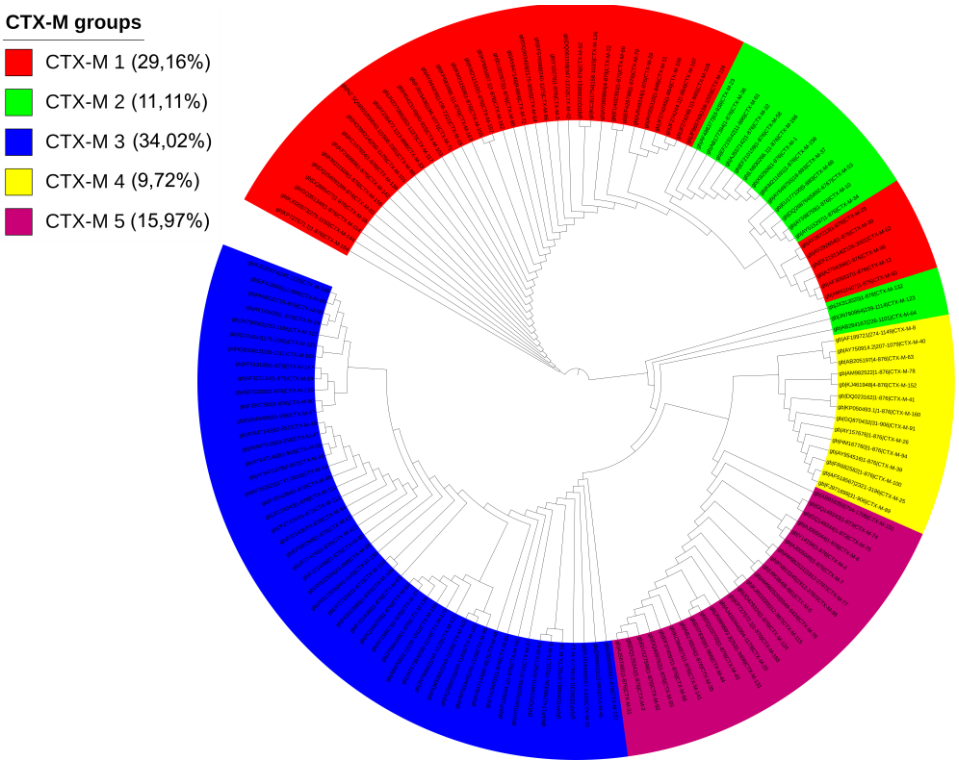

Figure 3. Cladogram with all sequences from the *blaCTX-M* subfamily divided into groups, illustrating the identifiable sequences, and the percentage of sequences detectable by each primer in comparison with the total number of the *blaCTX-M* family (N = 144) until the time of publication of this work.

medRxiv preprint doi: https://doi.org/10.1101/2023.12.30.23300671; this version posted December 31, 2023. The copyright holder for this preprint (which was not certified by peer review) is the author/funder, who has granted medRxiv a license to display the preprint in perpetuity.
It is made available under a CC-BY-ND 4.0 International license .

A total of 14 pairs of primers were developed, which together have the capacity to detect 740 variants of resistance genes belonging to the *bla* gene family. The primer sequences for genes with conserved and non-conserved sequences can be found in **Tables 1** and **2**, respectively.

Table 1. Primer sequences for conserved genes

Name of gene	Number of variations detectable	Name of primer	Sequence	Size primer
***bla*SHV**	156	SHV-F	ATTATCTCCCTGTTAGCCACCC	22
		SHV-R	GTTTAATTTGCTCAAGCGGCTG	22
***bla*TEM**	167	TEM-F	ACCCAGAAACGCTGGTGAAA	20
		TEM-R	GGGGCGAAAACTCTCAAGGA	20
***bla*NDM**	27	NDM-F	GAAGCTGAGCACCGCATTAG	20
		NDM-R	CCATTTGCTGGCCAATCGTC	20
***bla*KPC**	19	KPC-F	TCGCGGAACCATTCGCTAAA	20
		KPC-R	GAATGAGCTGCACAGTGGGA	20
***bla*GES**	25	GES-F	GCCCAGGAGAGAGATTACGC	20
		GES-R	CTTGACCGACAGAGGCAACT	20

Table 2. Primer sequences for non-conserved genes, divided into clades.

Name of gene		Number of variations detectable	Name of primer	Sequence	Size primer
***bla*CTX-M**	***bla*CTX-M 1**	42	CTXM-F1	GATTGCGGAAAAGCACGTCA	20
			CTXM-R1	TTCATCGCCACGTTATCGCT	20
	***bla*CTX-M 2**	16	CTXM-F2	CGCCGCTGATTCTGGTCA	18
			CTXM-R2	TGACGATTTTAGCCGCCGAC	20
	***bla*CTX-M 3**	49	CTXM-F3	CGTGGCTCAAAGGCAATACG	20
			CTXM-R3	TCTGTTGCGGCTGGGTAAAA	20
	***bla*CTX-M 4**	14	CTXM-F4	CGCTCAACACCGCGATCC	18
			CTXM-R4	ATCCCCGACAACCCACGAT	19
	***bla*CTX-M 5**	23	CTXM-F5	ATGGCGCAGACCCTGAAAAA	20
			CTXM-R5	CTGCCGGTTTTATCGCCCA	19
***bla*OXA**	***bla*OXA-23*like***	24	OXA23L-F	GCTCTAAGCCGCGCAAATAC	20
			OXA23L-R	TGACCTTTTCTCGCCCTTCC	20
	bla*OXA-24/40*like	8	OXA24/40L-F	TGCCGATGACCTTGCACATA	20
			OXA24/40L-R	CCATTAGCTTGCTCCACCCA	20
	bla*OXA-48*like	17	OXA48L-F	CGGTAGCAAAGGAATGGCAAG	21
			OXA48L-R	GGGCGATCAAGCTATTGGGA	20
	bla*OXA-51*like	153	OXA51L-F	GATCGGCCTTGAGCACCATA	20
			OXA51L-R	GCCATAACCAACACGCTTCA	20

medRxiv preprint doi: https://doi.org/10.1101/2023.12.30.23300671; this version posted December 31, 2023. The copyright holder for this preprint (which was not certified by peer review) is the author/funder, who has granted medRxiv a license to display the preprint in perpetuity.
It is made available under a CC-BY-ND 4.0 International license .

3.4. Validation of primers

3.4.1. *In silico* validation

The parameters obtained for each primer after analysis using the Primer-BLAST® (NCBI, USA) and Sequence Manipulation Suite (SMS): PCR Primer Stats software are available in **Table 3**.

Table 3. Parameters obtained by *in silico* validation of the developed primers.

Gene	Nome do primer	Tm (C°)	GC%	Self complementarity	Self 3' complementarity	Produt length
***bla*SHV**	SHV-F	59,2	50,0	3	0	70
	SHV-R	59,3	45,4	5	3	
***bla*TEM**	TEM-F	60,1	50,0	4	0	110
	TEM-R	59,9	55,0	2	1	
***bla*NDM**	NDM-F	59,3	55,0	5	1	86
	NDM-R	60,1	55,0	6	2	
***bla*KPC**	KPC-F	60,3	50,0	4	2	128
	KPC-R	60,3	55,0	5	1	
***bla*GES**	GES-F	59,9	60,0	3	2	94
	GES-R	59,9	55,0	3	2	
***bla*CTX-M 1**	CTXM-F1	59,7	50,0	4	1	87
	CTXM-R1	60,1	50,0	4	2	
***bla*CTX-M 2**	CTXM-F2	60,1	61,1	3	2	90
	CTXM-R2	61,0	55,0	3	3	
***bla*CTX-M 3**	CTXM-F3	59,9	55,0	3	2	180
	CTXM-R3	60,1	50,0	3	0	
***bla*CTX-M 4**	CTXM-F4	61,5	66,6	4	2	197
	CTXM-R4	60,9	57,8	3	2	
***bla*CTX-M 5**	CTXM-F5	60,5	50,0	4	0	155
	CTXM-R5	60,7	57,8	4	1	
bla*OXA-23*like	OXA23L-F	60,0	55,0	4	0	129
	OXA23L-R	59,9	55,0	2	0	
bla*OXA-24/40*like	OXA24/40L-F	59,7	50,0	4	2	177
	OXA24/40L-R	60,0	55,0	4	0	
bla*OXA-48*like	OXA48L-F	59,8	52,3	3	0	183
	OXA48L-R	59,8	55,0	4	0	
bla*OXA-51*like	OXA51L-F	59,8	55,0	4	2	199
	OXA51L-R	59,1	50,0	2	1	

3.4.2. Testing, optimization, and standardization of *in vitro* reactions.

All primers were tested using positive controls developed in-house, and it was possible to verify that the ideal annealing temperature (Ta) for the developed primer pairs was 61°C, except for the primer referring

medRxiv preprint doi: https://doi.org/10.1101/2023.12.30.23300671; this version posted December 31, 2023. The copyright holder for this preprint (which was not certified by peer review) is the author/funder, who has granted medRxiv a license to display the preprint in perpetuity.
It is made available under a CC-BY-ND 4.0 International license .

to the *blaNDM* gene, for which the ideal Ta was 64°C. The reactions were then evaluated for their specificity and stability by checking the Melting curve (Tm). The melting curves are available in the supplementary material Figure S3.

3.4.3. Efficiency curve

It was found that all tested primers presented an efficiency rate ⩾93.21 and ⩽101.28%, R^2 ⩾0.99, and detection limit between ≈2 and ≈13 copies/µL as shown in **Table 4**.

Table 4. Results of the efficiency curves of the developed primers.

Gene name	Efficiency (%)	Correlation coefficient (R^2)	Threshold	Detection limit (Copies/µL)	Melting Peak (Tm°C)
***bla*SHV**	96,15	0,992	0,60	≈2	86,7
***bla*TEM**	95,32	1,000	0,70	≈2	81,5
***bla*NDM**	99,90	0,999	0,48	≈2	85,7
***bla*KPC**	100,44	0,992	0,24	≈2	85,7
***bla*GES**	100,21	0,997	0,27	≈2	81,7
***bla*CTX-M 1**	95,75	0,999	0,40	≈13	84,3
***bla*CTX-M 2**	100,82	0,994	0,32	≈13	83,2
***bla*CTX-M 3**	97,82	0,996	0,10	≈2	89,0
***bla*CTX-M 4**	95,32	1,000	0,10	≈13	88,4
***bla*CTX-M 5**	98,09	0,998	0,30	≈2	86,4
bla*OXA-23*like	99,51	1,000	0,15	≈2	78,4
bla*OXA-24/40*like	101,82	0,988	0,15	≈13	78,7
bla*OXA-48*like	93,21	1,000	0,20	≈13	80,29
bla*OXA-51*like	95,51	0,993	0,55	≈2	82,0

medRxiv preprint doi: https://doi.org/10.1101/2023.12.30.23300671; this version posted December 31, 2023. The copyright holder for this preprint (which was not certified by peer review) is the author/funder, who has granted medRxiv a license to display the preprint in perpetuity.
It is made available under a CC-BY-ND 4.0 International license .

3.5. Identification of the genetic resistance profile of *K. pneumoniae* isolates

The 122 *K. pneumoniae* isolates were tested against the 14 pairs of primers developed, and it was possible to verify a high prevalence of beta-lactam resistance genes among the isolates analyzed. The most prevalent genes detected in the analyzed isolates were, respectively: *blaKPC* (95.90%); *blaSHV* (94.26%); *blaCTX-M* 2 (88.52%); *blaCTX-M* 5 (83.61%); *blaCTX-M* 1 (80.33%); *blaTEM* (80.33%); *blaNDM* (33.61%); *blaOXA-23like* (28.69%); *blaGES* (20.49%); *blaOXA-51like* (15.57%); *blaCTX-M* 3 (13.93%); *blaCTX-M* 4 (12.30%); *blaOXA-24/40like* (11.48%) and *blaOXA-48like* (3.28%). The results can be seen in **Figure 4**, grouped according to Ambler's *classification.*

Through the data obtained through the qPCR reactions developed, it was also possible to verify that the isolates analyzed during this study had the presence of several genes belonging to the *bla* family accumulated, with values varying from 3 to 12 of the tested genes, present per isolate, as shown in **Figure 5**.

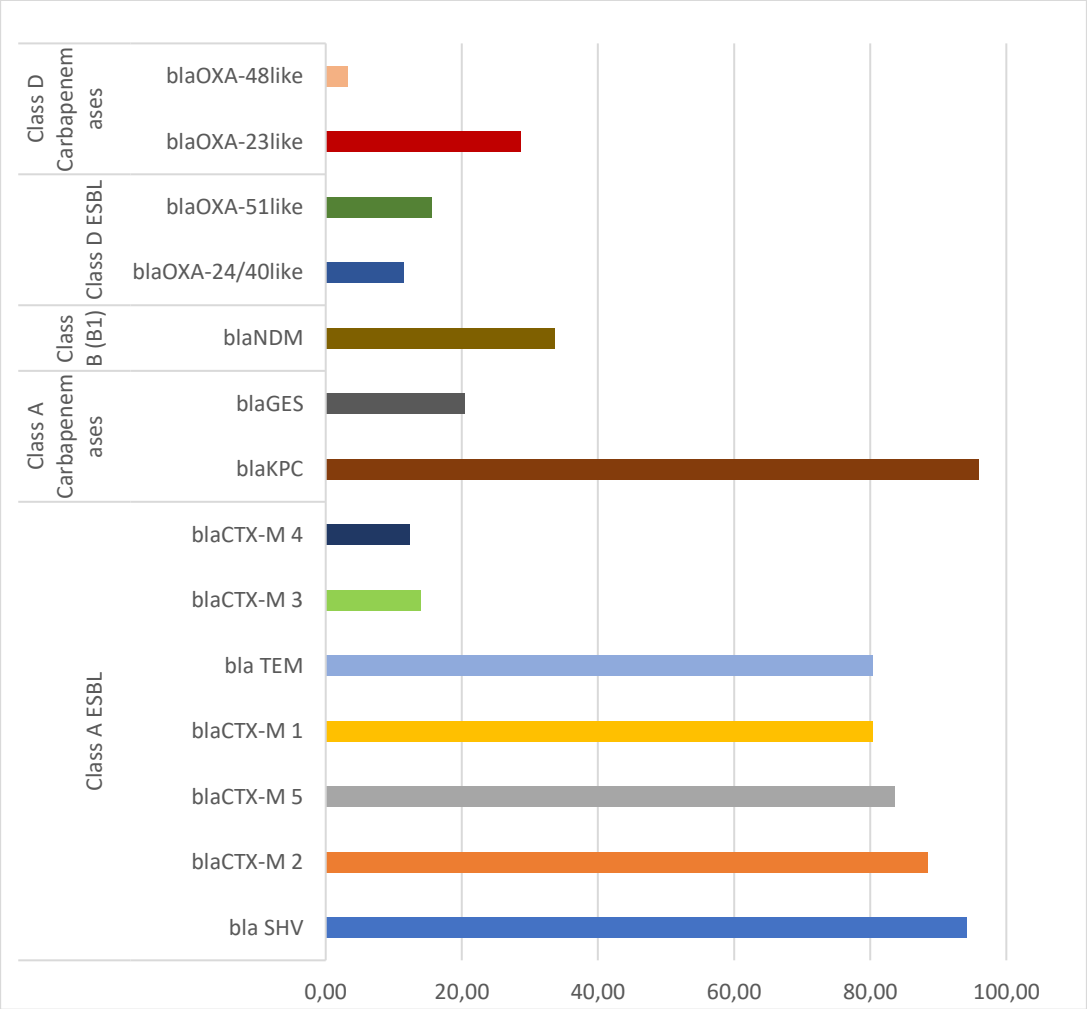

Figure 4. Prevalence of beta-lactams resistance genes among the analyzed isolates, grouped according to the Ambler classification, where it is possible to verify the presence of a high detection rate for class A ESBL (*blaSHV*; *blaCTX-M* of clade 2, 5 and 1 respectively; *blaTEM*), marked presence of the carbapenemase *blaKPC*, and the metallo beta-lactamase NDM, in addition to the identification of *blaOXA-24/40like*, *blaOXA-51like* and *blaOXA-23like*, commonly associated with *Acinetobacter baumannii* strains.

medRxiv preprint doi: https://doi.org/10.1101/2023.12.30.23300671; this version posted December 31, 2023. The copyright holder for this preprint **(which was not certified by peer review)** is the author/funder, who has granted medRxiv a license to display the preprint in perpetuity.
It is made available under a CC-BY-ND 4.0 International license .

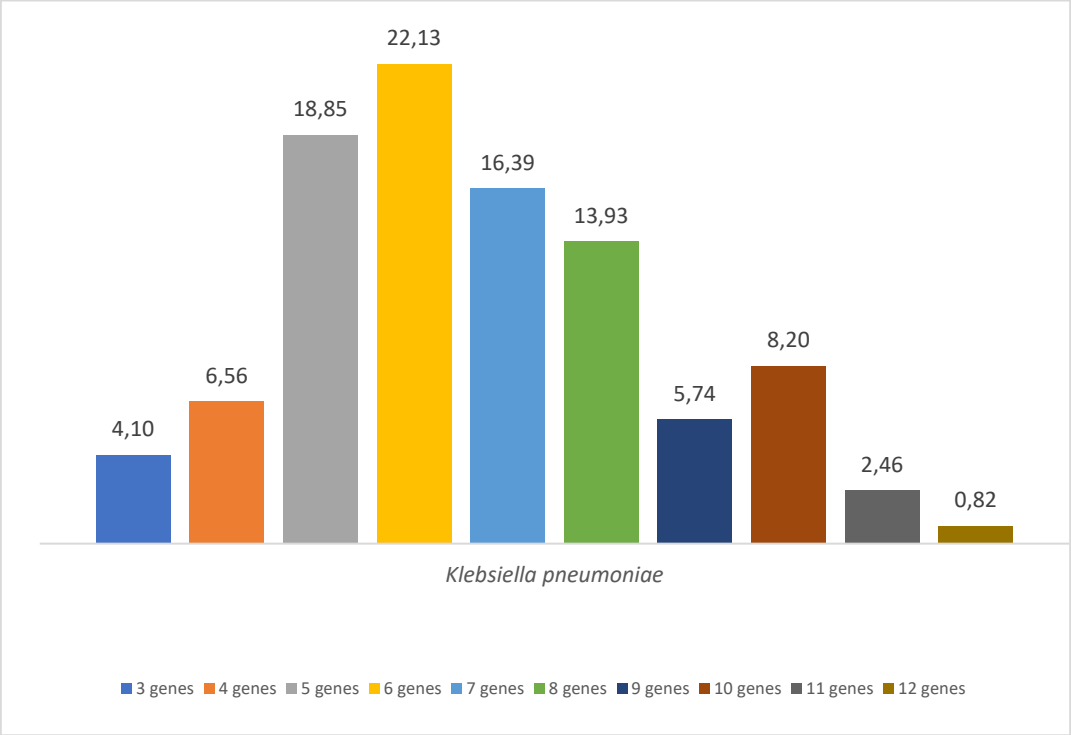

Figure 5. The percentage of *K. pneumoniae* isolates showing accumulation of genes encoding beta-lactamases belonging to the *bla* family. Where, it appears that among the 122 isolates evaluated, the majority of 22.13% present 6 of the genes evaluated in the study, demonstrating a high rate of sharing of these genes in the hospital environment.

3.6 Comparisons of metabolomic profiles between supernatants of susceptible or resistant *K. pneumoniae* versus the control culture media.

In total, 241 metabolites were identified in positive mode and 116 metabolites identified in negative mode. Of these, 309 metabolites were identified by combining data from both acquisition modes (positive and negative) without redundancy.

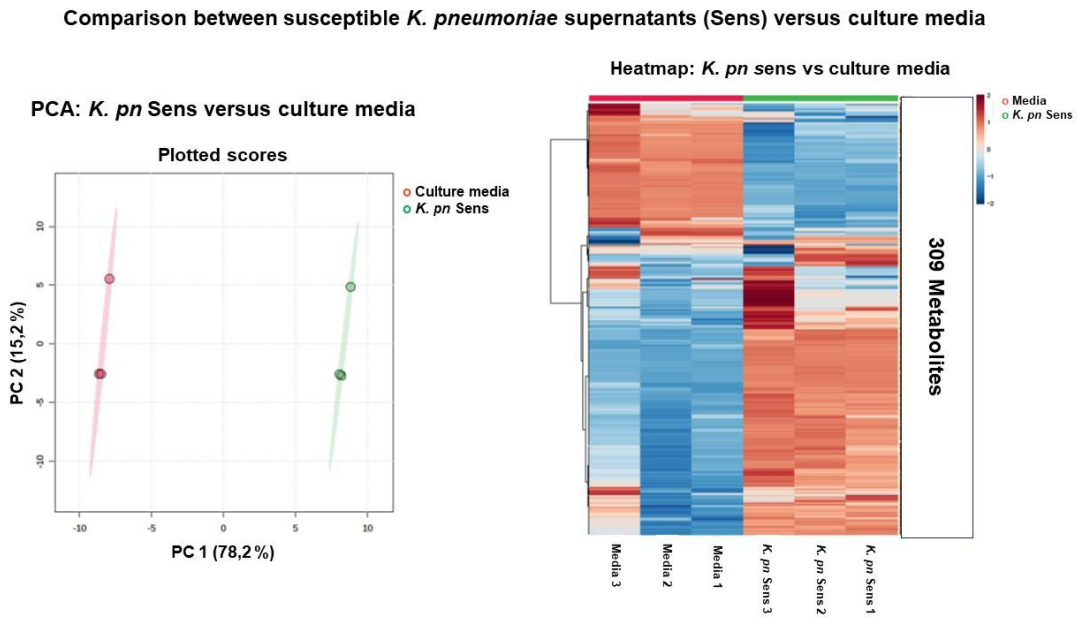

medRxiv preprint doi: https://doi.org/10.1101/2023.12.30.23300671; this version posted December 31, 2023. The copyright holder for this preprint **(which was not certified by peer review)** is the author/funder, who has granted medRxiv a license to display the preprint in perpetuity.
It is made available under a CC-BY-ND 4.0 International license .

Figure 6 - Plots of the principal component analysis (PCAs) and the heatmap of the comparison of metabolites between the supernatant of susceptible *K. pneumoniae* versus the control culture media. Observe the complete separation of the main vectors of the PCA plots and details of the differences in the heatmap between the two experimental groups.

Figure 6 shows the results using principal component analysis (PCAs) plots and the heatmap of the comparison of metabolites between the supernatant of sensitive K. pneumoniae versus the control culture medium. Observe the complete separation of the main vectors of the PCA plots and details of the differences in the heatmap between the two experimental groups. Figures S2, S3 and S4 show the analyzes of the 25 main metabolites analyzed, together and separated by up-regulated and down-regulated. Note that in the supernatant of susceptible K. pneumonia compared to the culture medium, metabolites related to the synthesis of nitrogenous bases, protein synthesis and energy supply to the bacterial cell are significantly increased.

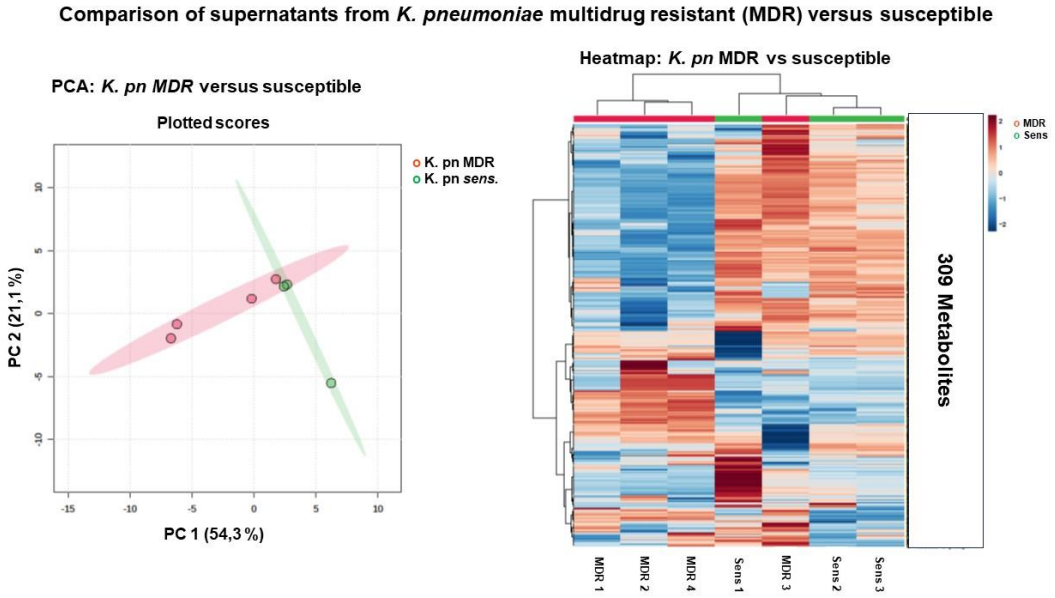

Figure 7 - Plots of the principal component analysis (PCAs) and the heatmap of the comparison of metabolites between the supernatant of *K. pneumoniae* MDR versus the control culture media. Note here also the complete separation of the main vectors of the PCA plots and details of the differences in the heatmap between the two experimental groups.

Figure 7 shows the results using principal component analysis (PCAs) plots and the heatmap for the comparison of metabolites between the K. pneumoniae MDR supernatant versus the control culture medium. Note here also the complete separation of the main vectors of the PCA plots and details of the differences in the heatmap between the two experimental groups. Figures S5, S6 and S7 show the analyzes now using the MDR *K. pneumoniae* strains compared to the control culture medium. Also note that in the supernatant of *K. pneumoniae* MDR, metabolites related to the synthesis of nitrogenous bases, protein synthesis and energy supply to the bacterial cell are significantly increased.

medRxiv preprint doi: https://doi.org/10.1101/2023.12.30.23300671; this version posted December 31, 2023. The copyright holder for this preprint (which was not certified by peer review) is the author/funder, who has granted medRxiv a license to display the preprint in perpetuity.
It is made available under a CC-BY-ND 4.0 International license .

3.7 Comparisons of metabolomic profiles between supernatants or intracellular media of susceptible versus resistant K. pneumoniae

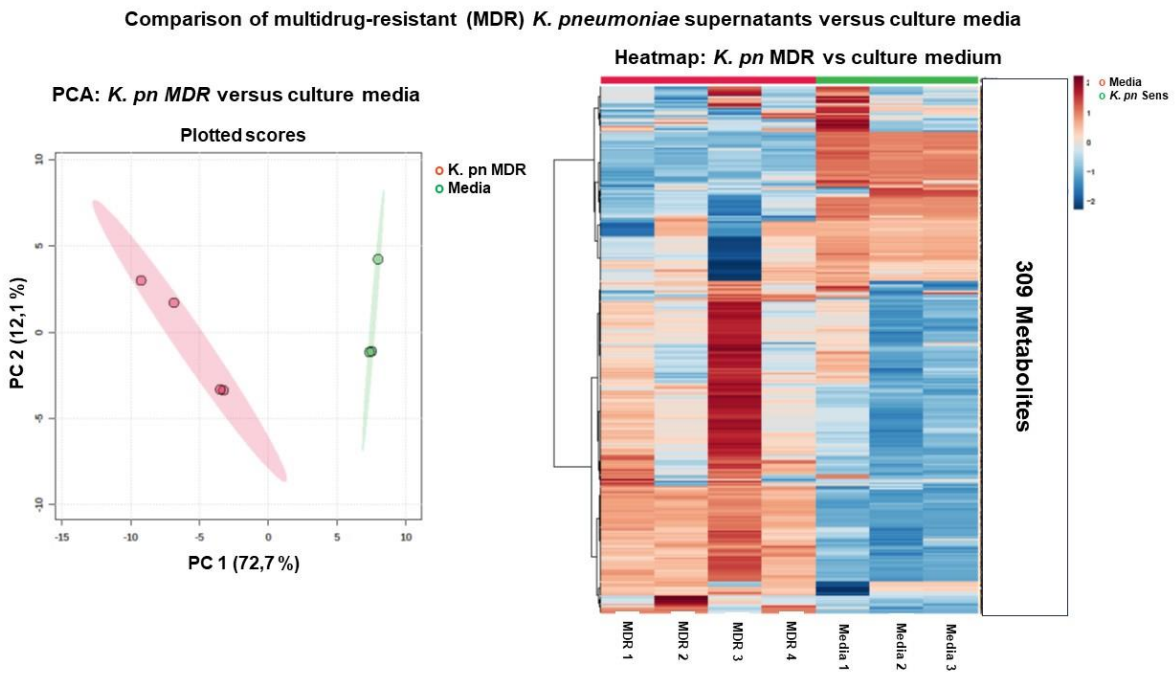

Figure 8 - Principal component analysis (PCAs) plots and heatmap of the supernatant of *K. pneumoniae* susceptible and MDR. Observe the separation of the main vectors of the (PCAs) plots and details of the differences in the heatmap between the two experimental groups.

Figure 8 shows the PCAs and heatmap plots of supernatant from sensitive and MDR *K. pneumoniae*.

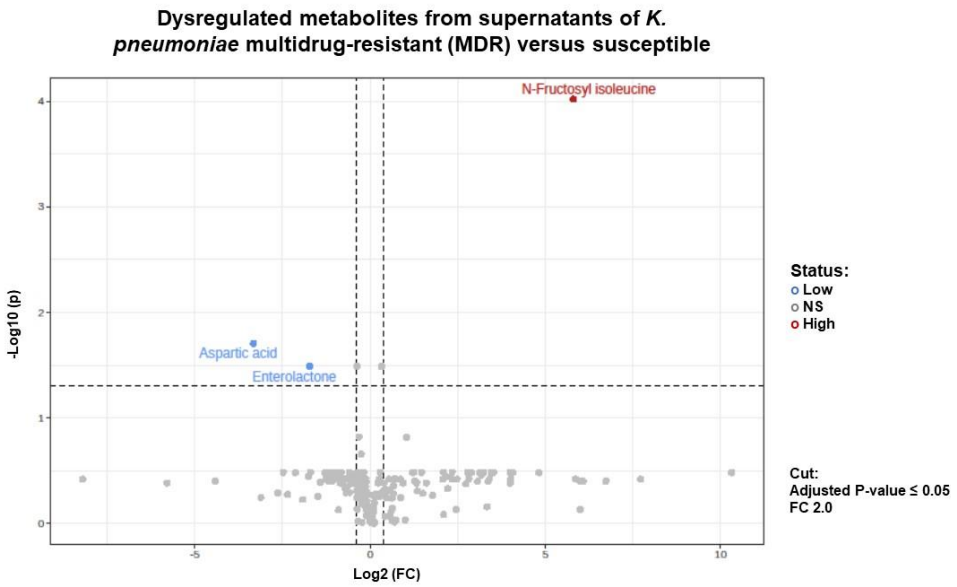

Figure 9 - Plots of dysregulated metabolites between supernatants of *K. pneumoniae* susceptible and MDR. Note that only one metabolite, N-fructosyl isoleucine, showed a significant increase ($p < 0.05$) in the MDR K. pneumoniae group.

medRxiv preprint doi: https://doi.org/10.1101/2023.12.30.23300671; this version posted December 31, 2023. The copyright holder for this preprint **(which was not certified by peer review)** is the author/funder, who has granted medRxiv a license to display the preprint in perpetuity.
It is made available under a CC-BY-ND 4.0 International license .

In **Figure 9** we observe the analysis of deregulated metabolites between these experimental groups. Note that only one metabolite, N-fructosyl isoleucine, showed a significant increase in the MDR K. pneumoniae group. Analysis of the intracellular media of susceptible versus MDR K. pneumoniae showed differences in the PCAs vectors, heatmap and that only the N-fructosyl metabolite isoleucine is significantly increased in the MDR K. pneumoniae group (**Figures 10** and **11**).

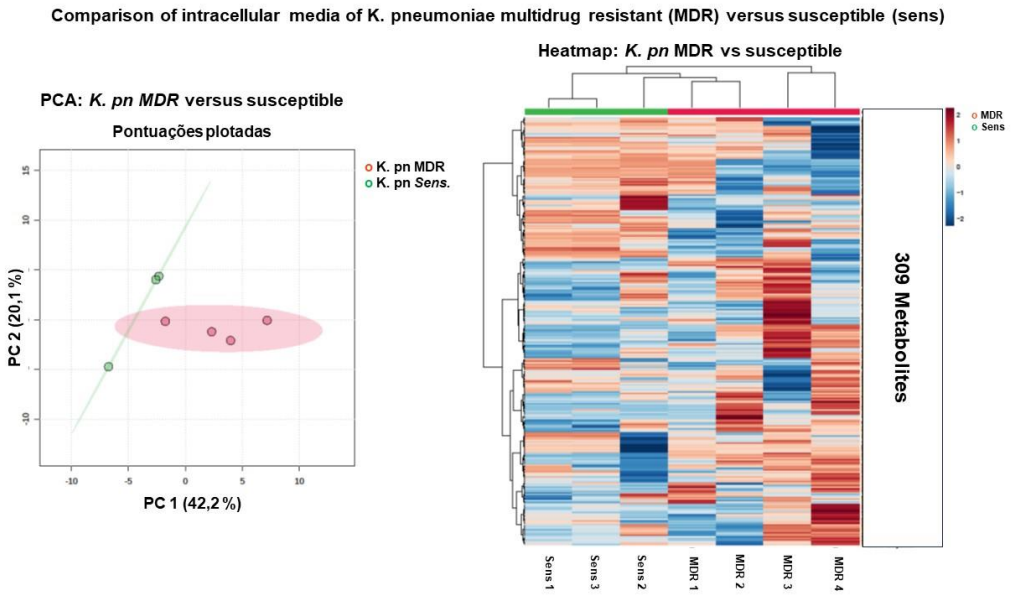

Figure 10 - Principal component analysis (PCAs) plots and heatmap of the intracellular environment of susceptible *K. pneumoniae* and MDR. Observe the separation of the main vectors of the (PCAs) plots and details of the differences in the heatmap between the two experimental groups.

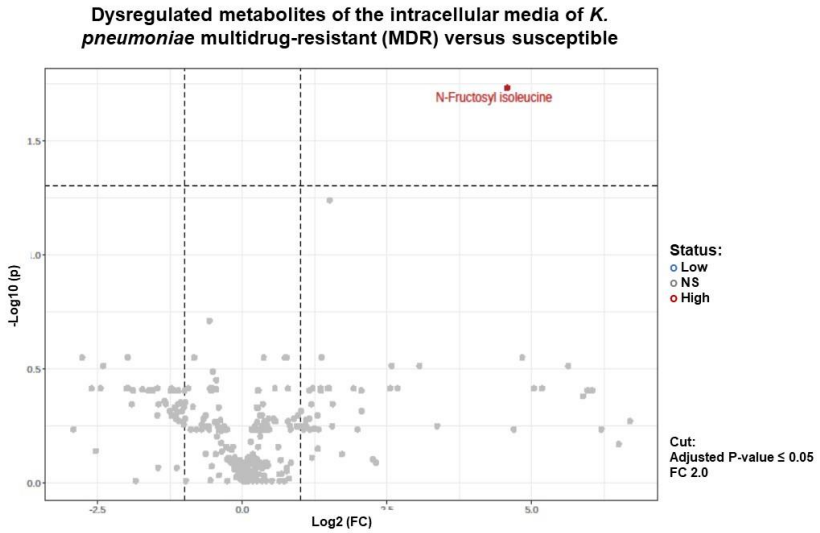

Figure 11 - Plots of dysregulated metabolites between the intracellular media of susceptible *K. pneumoniae* and MDR. Note that only one metabolite, N-fructosyl isoleucine, showed a significant increase ($p < 0.05$) in the MDR K. pneumoniae group.

medRxiv preprint doi: https://doi.org/10.1101/2023.12.30.23300671; this version posted December 31, 2023. The copyright holder for this preprint (which was not certified by peer review) is the author/funder, who has granted medRxiv a license to display the preprint in perpetuity.
It is made available under a CC-BY-ND 4.0 International license .

4. Discussion

During the period analyzed in the study, 249 bacterial isolates resistant to one or more of one class of antimicrobials used in TSA were identified. Of these resistant isolates, 48.99% (122/249) belonged to the species *Klebsiella pneumoniae*, meaning that this microorganism was the most prevalent among those identified.

This data is consistent with what is seen in Egypt, where when evaluating 186 samples from Cairo hospitals, *K. pneumoniae* was found as the main gram-negative bacterial agent representing 40.9% (76/186) of the identified microorganisms, and among these isolates obtained, a high prevalence of resistance to beta-lactams, quinolones, and sulfonamides was identified (89.4%, 89.4% and 87.1%) respectively [17]. The phenotypic profile of the *K. pneumoniae* isolates analyzed in the present study demonstrated high levels of resistance to the beta-lactams drugs tested in all classes evaluated (penicillins, cephalosporins and carbapenems). Although the resistance profile of strains may vary depending on the location and conditions to prevent the spread of resistance, the presence of resistance to beta-lactams among *Enterobacteriaceae* is reportedly high, as demonstrated in a study carried out in Brazil, with samples of human and veterinary origin where 74.28%, 62.85% and 54.28% of *Enterobacteriaceae* isolated were resistant to ampicillin, amoxicillin/clavulonate and cefazolin respectively [18].

In studies carried out in Egypt, evaluating isolates of *K. pneumoniae* from food sources, and in Tunisia evaluating isolates from hospital samples, the presence of high resistance to beta-lactams can be verified for ceftazidime (95.5%), cefoxitin (95.5%), cefotaxime (93.2%), amoxicillin/clavulonate (86.4%), ertapenem (90.9%) and temocillin (84.0%) [19, 20].

Likewise, in a study carried out with 102 isolates obtained from two Portuguese hospitals, the presence of resistance rates > 90% was verified for all beta-lactam drugs tested, except for cephalosporins: cefoxitin (40.2%), cefotetan (68.6%) and carbapenems: ertapenem (23.5%), imipenem (32.4%), meropenem (34.3%) and doripenem (33.3%) [21].

This result is consistent with that found in this study, where the beta-lactam drugs that showed a lower resistance rate belonged to the same classes mentioned, namely: cefoxitin (73.68%), ceftazidime/avibactam (11.76%), ertapenem (44.00%), imipenem (71.70%) and meropenem (69.81%).

Resistance to beta-lactams is conferred in gram negatives mainly by genes belonging to the *bla* family. This group of genes is composed of dozens of subfamilies and hundreds of genetic subvariants in each family, the molecular panel developed managed to encompass the most predominant subfamilies and clinically relevant among clinical isolates, identified in several studies, namely: *blaSHV*, *blaTEM*, *blaNDM*, *blaKPC*, *blaGES, blaCTX-M* and *blaOXA* [22, 23, 24]. After analysis using the Primer-BLAST® (NCBI, USA) and Primer Stats Sequence Manipulation Suite (SMS) software, it was verified that the developed primers have specificity for the sequences used in the alignment, melting temperature (Tm) between 59 29° C and 61.55° C, GC% concentration varying between 45.45% and 66.67% in addition to having complementary base numbers $\leqslant$ 6 in the analysis of dimer and hairpin formation. The values obtained for these parameters therefore demonstrate that they are compatible with those obtained in reference studies [25, 26, 27].

Due to the high number of sequences included in the development of primers, many of the alternatives obtained through Primer-BLAST® (NCBI, USA) did not meet the stability requirements regarding the formation of secondary structures (self-annealing and hairpins), In order to choose the options with the best performance in relation to these parameters, the GC clamp was relaxed so that the primers SHV-F, SHV-R, CTXM-R2 and CTXM-R5 obtained 4 G or C residues within the last 5 nucleotides of the 3' end, the primers CTXM-R3 and CTXM-F5 did not present C or G residues within the last 5 nucleotides of the sequence.

medRxiv preprint doi: https://doi.org/10.1101/2023.12.30.23300671; this version posted December 31, 2023. The copyright holder for this preprint **(which was not certified by peer review)** is the author/funder, who has granted medRxiv a license to display the preprint in perpetuity.
It is made available under a CC-BY-ND 4.0 International license .

This fact could lead to the formation of strong bonds and increase the Tm value in primers with more than 3 terminal GC residues, and cause inhibition of amplification due to the presence of weak bonds when there is an absence of terminal CG [26, 27]. Such changes, however, were not evident when the primers were tested *in vitro*.

The variety of sequences detectable by the developed primers makes in vitro validation using positive controls for all sequences virtually impossible. In silico analysis allowed the evaluation of all tested sequences quickly, cheaply, and constantly, since the developed primers can be tested against new variants of the target genes [26, 28].

In vitro analyzes were carried out using SYBR Green master mix, the melting curve was therefore used as a parameter to evaluate the specificity of the reactions. And it was verified that for all tested primers a single melting peak was found, indicating the formation of a single amplicon. And excluding the presence of secondary structures (primer dimers and hairpins).

The analysis of the melting curve and Tm is considered fundamental to test the specificity of reactions that use CYBR Green as an amplification indicator, because unlike reactions that use specific probes, which emit fluorescence only when the reaction occurs at the expected target. The CYBR Green works by binding to any double-stranded fragment formed, thus emitting fluorescence. Therefore, only by analyzing the melting curve and the specific Tm of the amplicon is it possible to determine whether the reaction was successful [29, 30, 31].

The efficiency curve and its parameters were used to evaluate the performance of qPCR reactions, by checking how efficiently the targets were amplified in each PCR cycle [32, 33]. When evaluating the activity of primers in qPCR reactions using the efficiency curve, it was found that all primers analyzed in this study presented efficiency values >90% and <110% and correlation coefficients (R^2) >0.9, thus being in accordance with the parameters presented in reference documents present in the literature [33]. It was also possible to verify a high detection capacity even at low concentrations of genetic material since the detection limit obtained varied between $\approx$2 and $\approx$13 copies/µL of the target gene used as control.

Several studies report the growth in the prevalence of the *blaKPC* gene, with carbapenemase being the most detected worldwide. The values found vary according to the location. The main variant of the *blaKPC* gene detected is *blaKPC-2*, with prevalence values varying from 1.2% to 51.6% among enterobacteria in studies carried out in the United States of America and China respectively [34, 35]. This gene is found more frequently in isolates of *K. pneumoniae*, studies report high prevalence rates in this species ranging from 17.2% to 64.6% [34, 36, 37, 38].

The higher values found in this study for the *blaKPC* gene may be the result of both the fact that the primer developed detected all variants of the gene, as well as the fact that the samples from which the isolates were obtained came from an intensive care unit (ICU), where It is known that infection and colonization rates by resistant microorganisms are higher, due to the high exposure of microorganisms to antimicrobials such as carbapenems and fluoroquinolones [39].

The *blaTEM* and *blaSHV* genes were the first ESBL identified, and together with the *blaCTX-M* subfamily of genes, they are considered the most prevalent ESBL. These genes are widely distributed among enterobacteria; in a study carried out in Sudan, the *blaTEM*, *blaCTX-M* and *blaSHV* genes were identified in 86.0%, 78.0% and 28.0% respectively [40].

In work carried out in ICUs in Chile, it was possible to verify the presence of these genes with prevalence rates of 81.0%, 84.7% and 73.0% for *blaSHV*, *blaCTX-M-1* and *blaTEM*, where a higher prevalence of the *blaSHV* gene compared to the study carried out in Sudan. These results agree with those evidenced in this study for the K. pneumoniae isolates tested [41].

medRxiv preprint doi: https://doi.org/10.1101/2023.12.30.23300671; this version posted December 31, 2023. The copyright holder for this preprint **(which was not certified by peer review)** is the author/funder, who has granted medRxiv a license to display the preprint in perpetuity.
It is made available under a CC-BY-ND 4.0 International license .

The *blaNDM* gene is considered the second most prevalent carbapene-mase producing gene in the world, behind only the *blaKPC* gene. In this study, the presence of the metallo beta-lactamase NDM was verified in (33.61%) of the isolates. Similar results were evidenced in China, where the presence of this gene was verified in 35.7% of 935 carbapenem-resistant enterobacteria tested [34].

Regarding oxacillinases, a low prevalence of the *blaOXA-48like* gene was observed (3.28%). This gene may be present in all *Enterobacteriaceae*; however, it is more prevalent in strains of *K. pneumoniae* [22].

The values found in the literature for the presence of this gene in *Enterobacteriaceae* are very divergent, with marked variations related to the location of the analysis, these values vary from 7.3% in China to 83.3% in Morocco [34, 42]. In a study conducted in Brazil where 4,451 isolates of *Enterobacteriaceae* were analyzed, the *blaOXA-48like* gene was detected in only 2.5% of the isolates tested [43]. In this way, the result obtained is compatible with what was previously identified in Brazil, and close to what is seen in China.

The presence of variants of the *blaOXA* gene (*bla-OXA-51like* (15.57%), *blaOXA-24/40like* (11.48%) and *blaOXA-23like* (28.69%)) was also observed in the isolates tested, these genes were long considered exclusive to strains of *Acinetobacter baumannii*, however studies have demonstrated the presence of these genes in other *Enterobacteriales*, including *K. pneumoniae* [44]. Results regarding the prevalence of these genes in strains of *K. pneumoniae* are still scarce, however, in a study conducted in Bahrain in the Persian Gulf, the *blaOXA-51* and *blaOXA-23* genes were identified respectively in 45.8% and 41.6%. % of *K. pneumoniae* isolates analyzed [45].

It is believed that many of the beta-lactamases that today can be found contained in mobile genetic elements had their origin in chromosomes of other bacteria, as occurred with the *SHV* type variants that derived from the *K. pneumoniae* chromosomal *SHV-1*, and the *CTX-M* type variants that appear to have originated from the chromosomal CTX-m of *Kluyvera* spp. [22]. This change in the presentation of these genes, from chromosomal to mobile elements, may explain the appearance of genes such as chromosomal *blaOXA* present in *A. baumannii* strains on plasmids widespread in other species.

It was possible to verify the presence of isolates presenting multiple genes coding for beta-lactamases, from 3 to 12 of the genes analyzed. Studies point to a high prevalence among *Enterobacteriaceae* of the accumulation of genes from the *bla* family, mainly genes belonging to ESBL, *OXA* beta-lactamases and carbapenemases such as *blaKPC* and *blaNDM*. This phenomenon is more evident in hospital environments where selective pressure favors microorganisms carrying resistance genes and where there is a high rate of sharing of these genes [46, 47].

Investigations into metabolomic modulation in *K. pneumoniae* have demonstrated a promising area for understanding resistance to antimicrobial agents, developing new therapies, and for studying bacterial virulence. For example, significant inhibition of the pentose phosphate pathway, citrate cycle, amino acid and nucleotide metabolism was observed to be beneficial during treatment of MDR *K. pneumoniae* using the bacteriophage-polymyxin combination, showing the potential for new therapeutic targets and pathways metabolic processes to improve the effectiveness of treatment with available antimicrobial agents [48, 49]. In this study, we highlighted the importance of the pentose phosphate pathway in MDR *K. pneumoniae* strains, in both isolates from supernatants and intracellular media, compared with *K. pneumoniae* strains susceptible to antimicrobial agents. The significant presence of the metabolic N-fructosyl isoleucine ($C_{12}H_{23}NO_7$; MW: 293.316) in the supernatant and intracellular media of *K. pneumoniae* MDR indicates the expression of the fructose degradation enzyme gene (*frwC*; fructose-specific phosphotransferase system), which is involved in regulating bacterial growth, virulence and overcoming colonization resistance due to the use of alternative carbon source from fructose [50, 51].

medRxiv preprint doi: https://doi.org/10.1101/2023.12.30.23300671; this version posted December 31, 2023. The copyright holder for this preprint **(which was not certified by peer review)** is the author/funder, who has granted medRxiv a license to display the preprint in perpetuity.
It is made available under a CC-BY-ND 4.0 International license .

This study has some limitations, such as the exploration of only *bla* family genes, limiting a broader understanding of resistance mechanisms to antimicrobial agents. On the other hand, it presents a broad methodology for exploring the important *bla* family genes most associated with resistance to beta-lactams in *K. pneumonia*. The metabolic findings showed a specific indication that suggests an association with virulence and better proteomic studies will be necessary to associate with potential mechanisms of resistance to antimicrobial agents. Furthermore, additional preclinical studies will be necessary to determine and more specifically validate the virulence associated with the pentose phosphate pathway in *K. pneumoniae*.

5. Conclusions

The results of this work show the high prevalence of resistance to antimicrobial agents in strains of *K. pneumoniae* within the hospital environment, and that this phenotypic pattern exhibited a great concern as it limits the therapeutic options available, directly implicating the patient's prognosis.

The assays developed were within the quality criteria for qPCR reactions using SYBR Green master mix and were efficient in detecting the beta-lactams resistance *bla* family genes evaluated in this study. The genotypes of the *bla* genes obtained are relevant and worrying for the local hospital scenario, and compatible with the identified phenotypic profile.

The identification of the metabolic N-fructosyl isoleucine in the supernatant and intracellular media of *K. pneumoniae* MDR indicates the expression of the fructose degradation enzyme gene, which is involved in regulating bacterial growth, virulence and overcoming resistance to colonization due to the use of an alternative carbon source from fructose.

Figure supplement legend

Figure S1 – Primer's specificity evaluation through Melting curve: (A) SHV, (B) KPC, (C) NDM, (D) TEM, (E) GES, (F) OXA-23, (G) OXA-24/40, (H) OXA-48, (I) OXA-51, (J) CTX-M 1, (K) CTX-M 2, (L) CTX-M 3, (M) CTX-M 4 e (N) CTX-M 5

Figure S2 - Plot analysis of the 25 main metabolites from the supernatant of susceptible K. pneumoniae in general without separation by up- or down-regulation of the analytes. Note that in the supernatant of K. pneumoniae compared to the culture media, metabolites related to the synthesis of nitrogenous bases, protein synthesis and energy supply to the bacterial cell are significantly increased.

Figure S3 - Plot of the analysis of the 25 main metabolites from the supernatant of susceptible K. pneumoniae, separated because they were up-regulated in relation to the control culture media.

Figure S4 - Plot of the analysis of the 25 main metabolites from the supernatant of susceptible K. pneumoniae, separated because they were down regulated in relation to the control culture media.

Figure S5 - Plot of the analyzes of the 25 main metabolites from the supernatant of multidrug resistant (MDR) K. pneumoniae in general without separation by up- or down-regulation in the analytes. Note that in the intracellular media of K. pneumoniae compared to the culture medium, metabolites related to the synthesis of nitrogenous bases, protein synthesis and energy supply to the bacterial cell are significantly increased.

Figure S6 - Plot of the analysis of the 25 main metabolites from the supernatant of K. pneumoniae MDR, separated by being up-regulated in relation to the control culture media.

Figure S7 - Plot d of the analysis of the 25 main metabolites from the supernatant of K. pneumoniae MDR, separated because they were down-regulated in relation to the control culture media.

medRxiv preprint doi: https://doi.org/10.1101/2023.12.30.23300671; this version posted December 31, 2023. The copyright holder for this preprint **(which was not certified by peer review)** is the author/funder, who has granted medRxiv a license to display the preprint in perpetuity.
It is made available under a CC-BY-ND 4.0 International license .

Author Contributions:

Bibliographic review and data collection, Lavouisier F.B. Nogueira, Marília S. Maia, Marco A.F Clementino and Aldo A.M. Lima; **Methodology**, Lavoui-sier F.B. Nogueira, Marília S. Maia, Marco A.F Clementino, Alexandre Havt, Ila F.N. Lima, Jorge L.N. Rodrigues, Luciana V. C. Fragoso and Aldo A. M. Lima; **Bioinformatics**, Lavouisier F.B. Nogueira and Marco A.F Clementino; **In silico analyses**, Lavouisier F.B. Nogueira, Marco A.F Clementino; ***In vitro* validation of primers and sample testing**, Lavouisier F.B. Nogueira, Marília S. Maia; **Metabolomics, Datascience and data Bank**, Jose Q.S. Filho; Deiziane V.S. Costa, José K. Sousa, Lyvia M.V.C. Magalhães, Dilza Silva, Nicholas E. Sherman and Aldo A.M. Lima; **Written review and editing**, Lavouisier F.B. Nogueira; Aldo A.M. Lima; **Supervision**, Alexandre Havt and Aldo A.M. Lima; **Project administration**, Aldo A.M. Lima; **Resource acquisition**, Aldo A.M. Lima.

Funding: This research was funded by CNPq (http://www.cnpq.br), grant numbers 402607/2018-0 and 408549/2022-0 and FUNCAP (https://www.funcap.ce.gov.br/), grant number: OFÍCIO Nº 102/2021 – DINOV.

Data Availability Statement: The data and reports relating to this study will be available via direct request via email to the corresponding author.

Conflicts of Interest: The authors declare that there are no financial or personal conflicts of interest that may have influenced the work.

medRxiv preprint doi: https://doi.org/10.1101/2023.12.30.23300671; this version posted December 31, 2023. The copyright holder for this preprint **(which was not certified by peer review)** is the author/funder, who has granted medRxiv a license to display the preprint in perpetuity.
It is made available under a CC-BY-ND 4.0 International license .

References

1. Munita, J.M.; Arias, C.A. Mechanisms of Antibiotic Resistance. *Microbiology Spectrum***2016**, *4*, doi:10.1128/microbiolspec.vmbf-0016-2015.
2. Frieri, M.; Kumar, K.; Boutin, A. Antibiotic Resistance. *Journal of Infection and Public Health***2017**, *10*, 369–378, doi:10.1016/j.jiph.2016.08.007.
3. Holt, K.E.; Wertheim, H.; Zadoks, R.N.; Baker, S.; Whitehouse, C.A.; Dance, D.; Jenney, A.; Connor, T.R.; Hsu, L.Y.; Severin, J.; et al. Genomic Analysis of Diversity, Population Structure, Virulence, and Antimicrobial Resistance in *Klebsiella Pneumoniae* , an Urgent Threat to Public Health. *Proceedings of the National Academy of Sciences***2015**, *112*, doi:10.1073/pnas.1501049112.
4. Mohd Asri, N.A.; Ahmad, S.; Mohamud, R.; Mohd Hanafi, N.; Mohd Zaidi, N.F.; Irekeola, A.A.; Shueb, R.H.; Yee, L.C.; Mohd Noor, N.; Mustafa, F.H.; et al. Global Prevalence of Nosocomial Multidrug-Resistant *Klebsiella Pneumoniae*: A Systematic Review and Meta-Analysis. *Antibiotics***2021**, *10*, 1508, doi:10.3390/antibiotics10121508.
5. Sharma, A.; Thakur, A.; Thakur, N.; Kumar, V.; Chauhan, A.; Bhardwaj, N. Changing Trend in the Antibiotic Resistance Pattern of *Klebsiella Pneumonia* Isolated From Endotracheal Aspirate Samples of ICU Patients of a Tertiary Care Hospital in North India. *Cureus***2023**, doi:10.7759/cureus.36317.
6. Cortés, G.; Borrell, N.; de Astorza, B.; Gómez, C.; Sauleda, J.; Albertí, S. Molecular Analysis of the Contribution of the Capsular Polysaccharide and the Lipopolysaccharide O Side Chain to the Virulence of Klebsiella Pneumoniae in a Murine Model of Pneumonia. *Infection and Immunity***2002**, *70*, 2583–2590, doi:10.1128/iai.70.5.2583-2590.2002.
7. Struve, C.; Bojer, M.; Krogfelt, K.A. Identification of a Conserved Chromosomal Region Encoding Klebsiella Pneumoniae Type 1 and Type 3 Fimbriae and Assessment of the Role of Fimbriae in Pathogenicity. *Infection and Immunity***2009**, *77*, 5016–5024, doi:10.1128/iai.00585-09.
8. Lin, C.-T.; Chen, Y.-C.; Jinn, T.-R.; Wu, C.-C.; Hong, Y.-M.; Wu, W.-H. Role of the cAMP-Dependent Carbon Catabolite Repression in Capsular Polysaccharide Biosynthesis in Klebsiella Pneumoniae. *PLoS ONE***2013**, *8*, e54430, doi:10.1371/journal.pone.0054430.
9. Davies, J.; Davies, D. Origins and Evolution of Antibiotic Resistance. *Microbiology and Molecular Biology Reviews***2010**, *74*, 417–433, doi:10.1128/mmbr.00016-10.
10. Salipante, S.J.; Jerome, K.R. Digital PCR—An Emerging Technology with Broad Applications in Microbiology. *Clinical Chemistry***2019**, *66*, 117–123, doi:10.1373/clinchem.2019.304048.
11. Bush, K.; Bradford, P.A. β-Lactams and β-Lactamase Inhibitors: An Overview. *Cold Spring Harbor Perspectives in Medicine***2016**, 6, a025247, doi:10.1101/cshperspect.a025247.
12. Ferreira, A.M.; Martins, K.B.; Silva, V.R. da; Mondelli, A.L.; Cunha, M. de L.R. de S. da Correlation of Phenotypic Tests with the Presence of the blaZ Gene for Detection of Beta-Lactamase. *Brazilian Journal of Microbiology***2017**, *48*, 159–166, doi:10.1016/j.bjm.2016.10.011.
13. Zhu, L.-J.; Pan, Y.; Gao, C.-Y.; & Hou, P.-F. (2020). Distribution of Carbapenemases and Efflux Pump in Carbapenem-resistance Acinetobacter baumannii. *Annals of Clinical and Laboratory Science* **2020**, *50*(2), 241–246.
14. Agência Nacional de Vigilância Sanitária (ANVISA). Procedimentos Laboratoriais: da Requisição do Exame à Análise Microbiológica e Laudo Final. 2. ed. Brasil: **2013**. Módulo 4.
15. Tsugawa, H.; Cajka, T.; Kind, T.; Ma, Y.; Higgins, B.; Ikeda, K.; Kanazawa, M.; VanderGheynst, J.; Fiehn, O.; Arita, M. MS-DIAL: Data-Independent MS/MS Deconvolution for Comprehensive Metabolome Analysis. *Nature Methods***2015**, *12*, 523–526, doi:10.1038/nmeth.3393.
16. Tsugawa, H.; Nakabayashi, R.; Mori, T.; Yamada, Y.; Takahashi, M.; Rai, A.; Sugiyama, R.; Yamamoto, H.; Nakaya, T.; Yamazaki, M.; et al. A Cheminformatics Approach to Characterize Metabolomes in Stable-Isotope-Labeled Organisms. *Nature Methods***2019**, *16*, 295–298, doi:10.1038/s41592-019-0358-2.
17. Makharita, R.R.; El-kholy, I.; Hetta, H.F.; Abdelaziz, M.; Hagagy, F.; Ahmed, A.; Algammal, A.M. <P>Antibiogram and Genetic Characterization of Carbapenem-Resistant Gram-Negative Pathogens Incriminated in Healthcare-Associated Infections</P> *Infection and Drug Resistance***2020**, *Volume 13*, 3991–4002, doi:10.2147/idr.s276975.

medRxiv preprint doi: https://doi.org/10.1101/2023.12.30.23300671; this version posted December 31, 2023. The copyright holder for this preprint **(which was not certified by peer review)** is the author/funder, who has granted medRxiv a license to display the preprint in perpetuity.
It is made available under a CC-BY-ND 4.0 International license .

18. Santos, A.L.; dos Santos, A.P.; Ito, C.R.M.; Queiroz, P.H.P. de; de Almeida, J.A.; de Carvalho Júnior, M.A.B.; de Oliveira, C.Z.; Avelino, M.A.G.; Wastowski, I.J.; Gomes, G.P.L.A.; et al. Profile of Enterobacteria Resistant to Beta-Lactams. *Antibiotics***2020**, *9*, 410, doi:10.3390/antibiotics9070410.
19. Abdel-Rhman, S.H. Characterization of β-Lactam Resistance in *K. Pneumoniae* Associated with Ready-to-Eat Processed Meat in Egypt. *PLOS ONE***2020**, *15*, e0238747, doi:10.1371/journal.pone.0238747.
20. Messaoudi, A.; Mansour, W.; Jaidane, N.; Chaouch, C.; Boujaâfar, N.; Bouallègue, O. Epidemiology of Resistance and Phenotypic Characterization of Carbapenem Resistance Mechanisms in *Klebsiella Pneumoniae* Isolates at Sahloul University Hospital-Sousse, Tunisia. *African Health Sciences***2019**, *19*, 2008, doi:10.4314/ahs.v19i2.24.
21. Oliveira, R.; Castro, J.; Silva, S.; Oliveira, H.; Saavedra, M.J.; Azevedo, N.F.; Almeida, C. Exploring the Antibiotic Resistance Profile of Clinical *Klebsiella Pneumoniae* Isolates in Portugal. *Antibiotics***2022**, *11*, 1613, doi:10.3390/antibiotics11111613.
22. Bush, K.; Bradford, P.A. Epidemiology of β-Lactamase-Producing Pathogens. *Clinical Microbiology Reviews***2020**, *33*, doi:10.1128/cmr.00047-19.
23. Castanheira, M.; Simner, P.J.; Bradford, P.A. Extended-Spectrum β-Lactamases: An Update on Their Characteristics, Epidemiology and Detection. *JAC-Antimicrobial Resistance***2021**, *3*, doi:10.1093/jacamr/dlab092.
24. Gundran, R.S.; Cardenio, P.A.; Villanueva, M.A.; Sison, F.B.; Benigno, C.C.; Kreausukon, K.; Pichpol, D.; Punyapornwithaya, V. Prevalence and Distribution of blaCTX-M, blaSHV, blaTEM Genes in Extended- Spectrum β- Lactamase- Producing E. Coli Isolates from Broiler Farms in the Philippines. *BMC Veterinary Research***2019**, *15*, doi:10.1186/s12917-019-1975-9.
25. Queiroz J.A.S.; Alves L.S.; Dall'acqua D.S.V.; Sousa L.F.B. Desenho e Validação de Primers In Silico para Detecção do Vírus Sincicial Respiratório Humano. *Revista FIMCA***2017**, 4(1), 17-30.
26. Kumar, A.; Chordia, N. In Silico PCR Primer Designing and Validation. In *Methods in Molecular Biology*; Springer New York: New York, NY**2015**; pp. 143–151.
27. Rodríguez, A.; Rodríguez, M.; Córdoba, J.J.; Andrade, M.J. Design of Primers and Probes for Quantitative Real-Time PCR Methods. In *Methods in Molecular Biology*; Springer New York: New York, NY**2015**; pp. 31–56.
28. van Weezep, E.; Kooi, E.A.; van Rijn, P.A. PCR Diagnostics: In Silico Validation by an Automated Tool Using Freely Available Software Programs. *Journal of Virological Methods***2019**, *270*, 106–112, doi:10.1016/j.jviromet.2019.05.002.
29. Yang, J.; Kemps-Mols, B.; Spruyt-Gerritse, M.; Anholts, J.; Claas, F.; Eikmans, M. The Source of SYBR Green Master Mix Determines Outcome of Nucleic Acid Amplification Reactions. *BMC Research Notes***2016**, *9*, doi:10.1186/s13104-016-2093-4.
30. Wang, Y.; Li, W.; Guo, X.; Zhang, D.; Sun, J.; Fu, Z.; Liu, G.; Li, Y.; Jiang, S. Development of SYBR Green I-Based Polymerase Chain Reaction for Feline Bocavirus 1 Detection. *3 Biotech***2021**, *11*, doi:10.1007/s13205-020-02577-8.
31. Desriani; Azamris; Ghaissani, S.S.; Kinanti, S.R.; Warisman, M.A.; Fitria, N. Design and Characterization of a SYBR Green I-Based Melting Curve Method for Investigation of HER2I655V Polymorphism in Breast Cancer. *Journal of Genetic Engineering and Biotechnology***2021**, *19*, doi:10.1186/s43141-020-00108-9.
32. Svec, D.; Tichopad, A.; Novosadova, V.; Pfaffl, M.W.; Kubista, M. How Good Is a PCR Efficiency Estimate: Recommendations for Precise and Robust qPCR Efficiency Assessments. *Biomolecular Detection and Quantification***2015**, *3*, 9–16, doi:10.1016/j.bdq.2015.01.005.
33. Thermo Fisher Scientific. Real-time PCR: understanding Ct. Available online: https://www.thermofisher.com/content/dam/LifeTech/global/Forms/PDF/real-time-pcr-handbook.pdf. (accessed on 03/12/2023).
34. Han, R.; Shi, Q.; Wu, S.; Yin, D.; Peng, M.; Dong, D.; Zheng, Y.; Guo, Y.; Zhang, R.; Hu, F. Dissemination of Carbapenemases (KPC, NDM, OXA-48, IMP, and VIM) Among Carbapenem-Resistant Enterobacteriaceae Isolated From Adult and Children Patients in China. *Frontiers in Cellular and Infection Microbiology***2020**, *10*, doi:10.3389/fcimb.2020.00314.
35. Marschall, J.; Tibbetts, R.J.; Dunne, W.M., Jr.; Frye, J.G.; Fraser, V.J.; Warren, D.K. Presence of the KPC Carbapenemase Gene in Enterobacteriaceae Causing Bacteremia and Its Correlation with In Vitro Carbapenem Susceptibility. *Journal of Clinical Microbiology***2009**, *47*, 239–241, doi:10.1128/jcm.02123-08.

medRxiv preprint doi: https://doi.org/10.1101/2023.12.30.23300671; this version posted December 31, 2023. The copyright holder for this preprint **(which was not certified by peer review)** is the author/funder, who has granted medRxiv a license to display the preprint in perpetuity.
It is made available under a CC-BY-ND 4.0 International license .

36. Kharazmkia, A.; Amirizadeh, M.; Goudarzi, Z.; Birjandi, M.; Barfipoursalar, A.; Mir, S. Prevalence of KPC-Producing Bacteria in Negative Gram of Clinical Samples Obtained from Patients. *Annals of Medicine & Surgery***2022**, *77*, doi:10.1016/j.amsu.2022.103690.
37. Pawłowska, I.; Ziółkowski, G.; Jachowicz-Matczak, E.; Stasiowski, M.; Gajda, M.; Wójkowska-Mach, J. Colonization and Healthcare-Associated Infection of Carbapenem-Resistant Enterobacteriaceae, Data from Polish Hospital with High Incidence of Carbapenem-Resistant Enterobacteriaceae, Does Active Target Screening Matter? *Microorganisms***2023**, *11*, 437, doi:10.3390/microorganisms11020437.
38. Mohd Asri, N.A.; Ahmad, S.; Mohamud, R.; Mohd Hanafi, N.; Mohd Zaidi, N.F.; Irekeola, A.A.; Shueb, R.H.; Yee, L.C.; Mohd Noor, N.; Mustafa, F.H.; et al. Global Prevalence of Nosocomial Multidrug-Resistant *Klebsiella Pneumoniae*: A Systematic Review and Meta-Analysis. *Antibiotics***2021**, *10*, 1508, doi:10.3390/antibiotics10121508.
39. Kernéis, S.; Lucet, J.C.; Santoro, A.; Meschiari, M. Individual and Collective Impact of *Klebsiella Pneumoniae* Carbapenemase (KPC)-Producing *K. Pneumoniae* in Patients Admitted to the ICU. *Journal of Antimicrobial Chemotherapy***2021**, *76*, i19–i26, doi:10.1093/jac/dkaa494.
40. Dirar, M.H.; Bilal, N.E.; Ibrahim, M.E.; Hamid, M.E. Prevalence of Extended-Spectrum β-Lactamase (ESBL) and Molecular Detection of Bla TEM, Bla SHV and Bla CTX-M Genotypes among Enterobacteriaceae Isolates from Patients in Khartoum, Sudan. *Pan African Medical Journal***2020**, *37*, doi:10.11604/pamj.2020.37.213.24988.
41. Pavez, M.; Troncoso, C.; Osses, I.; Salazar, R.; Illesca, V.; Reydet, P.; Rodríguez, C.; Chahin, C.; Concha, C.; Barrientos, L. High Prevalence of CTX-M-1 Group in ESBL-Producing Enterobacteriaceae Infection in Intensive Care Units in Southern Chile. *The Brazilian Journal of Infectious Diseases***2019**, *23*, 102–110, doi:10.1016/j.bjid.2019.03.002.
42. Belouad, E.M.; Benaissa, E.; El Mrimar, N.; Bssaibis, F.; Maleb, A.; Elouennass, M. Predominance of OXA-48 Carbapenemase-Producing Enterobacterales in a Moroccan Hospital. *International Journal of Microbiology***2023**, *2023*, 1–10, doi:10.1155/2023/8581883.
43. Magagnin, C.M.; Rozales, F.P.; Antochevis, L.; Nunes, L.S.; Martins, A.S.; Barth, A.L.; Sampaio, J.M.; Zavascki, A.P. Dissemination of Bla OXA-370 Gene among Several Enterobacteriaceae Species in Brazil. *European Journal of Clinical Microbiology & Infectious Diseases***2017**, *36*, 1907–1910, doi:10.1007/s10096-017-3012-x.
44. Evans, B.A.; Amyes, S.G.B. OXA β-Lactamases. *Clinical Microbiology Reviews***2014**, *27*, 241–263, doi:10.1128/cmr.00117-13.
45. Shahid, M.; Ahmad, N.; Saeed, N.K.; Shadab, M.; Joji, R.M.; Al-Mahmeed, A.; Bindayna, K.M.; Tabbara, K.S.; Dar, F.K. Clinical Carbapenem-Resistant *Klebsiella Pneumoniae* Isolates Simultaneously Harboring blaNDM-1, blaOXA Types and qnrS Genes from the Kingdom of Bahrain: Resistance Profile and Genetic Environment. *Frontiers in Cellular and Infection Microbiology***2022**, 12, doi:10.3389/fcimb.2022.1033305.
46. Manandhar, S.; Zellweger, R.M.; Maharjan, N.; Dongol, S.; Prajapati, K.G.; Thwaites, G.; Basnyat, B.; Dixit, S.M.; Baker, S.; Karkey, A. A High Prevalence of Multi-Drug Resistant Gram-Negative Bacilli in a Nepali Tertiary Care Hospital and Associated Widespread Distribution of Extended-Spectrum Beta-Lactamase (ESBL) and Carbapenemase-Encoding Genes. Annals of Clinical Microbiology and Antimicrobials2020, 19, doi:10.1186/s12941-020-00390-y.
47. Awosile, B.B.; Agbaje, M.; Adebowale, O.; Kehinde, O.; Omoshaba, E. Beta-Lactamase Resistance Genes in Enterobacteriaceae from Nigeria. African Journal of Laboratory Medicine2022, 11, doi:10.4102/ajlm.v11i1.1371.
48. Han, M.-L.; Nang, S.C.; Lin, Y.-W.; Zhu, Y.; Yu, H.H.; Wickremasinghe, H.; Barlow, C.K.; Creek, D.J.; Crawford, S.; Rao, G.; et al. Comparative Metabolomics Revealed Key Pathways Associated with the Synergistic Killing of Multidrug-Resistant Klebsiella Pneumoniae by a Bacteriophage-Polymyxin Combination. *Computational and Structural Biotechnology Journal***2022**, *20*, 485–495, doi:10.1016/j.csbj.2021.12.039.
49. Kumar, A.; Singh, S.; Gupta, S.K.; Kumar, S.; Kumar, S.; Singh, R.; Thakur, L.; Kumar, M.; Kapil, A.; Kumar, Y.; et al. Identification of Metabolite Extraction Method for Targeted Exploration of Antimicrobial Resistance Associated Metabolites of Klebsiella Pneumoniae. *Scientific Reports***2022**, *12*, doi:10.1038/s41598-022-12153-0.

medRxiv preprint doi: https://doi.org/10.1101/2023.12.30.23300671; this version posted December 31, 2023. The copyright holder for this preprint **(which was not certified by peer review)** is the author/funder, who has granted medRxiv a license to display the preprint in perpetuity.
It is made available under a CC-BY-ND 4.0 International license .

50. Hudson, A.W.; Barnes, A.J.; Bray, A.S.; Ornelles, D.A.; Zafar, M.A. Klebsiella Pneumoniae L- Fucose Metabolism Promotes Gastrointestinal Colonization and Modulates Its Virulence Determinants. *Infection and Immunity* **2022**, *90*, doi:10.1128/iai.00206-22.
51. Lin, D.; Fan, J.; Wang, J.; Liu, L.; Xu, L.; Li, F.; Yang, J.; Li, B. The Fructose-Specific Phosphotransferase System of Klebsiella Pneumoniae Is Regulated by Global Regulator CRP and Linked to Virulence and Growth. *Infection and Immunity* **2018**, *86*, doi:10.1128/iai.00340-18.